ORDER AND CHAOS IN MULTI–DIMENSIONAL HAMILTONIAN SYSTEMS

Tassos BOUNTIS

Haris SKOKOS, Eleni CHRISTODOULIDI and Thanos MANOS

Department of Mathematics and Center for Research and Applications of Nonlinear Systems (CRANS), University of Patras, Patras, Greece

1st Ph.D. School on "Mathematical Modeling of Complex Systems"

18 - 29 July 2011, Patras, Greece

Part I

Detecting Chaos, Determining the Dimensions of Tori and Predicting Slow Diffusion by the GALI METHOD

Contents

N–Degree– of–Freedom Hamiltonian Lattices

The Fermi–Pasta–Ulam (FPU) model and other Hamiltonians

We consider conservative systems described by an N - degree - of freedom Hamiltonian function of the form:

$$H \equiv H(q_1(t), \ldots, q_N(t), p_1(t), \ldots, p_N(t)) = E \tag{1}$$

where E is the total (constant) energy and the positions $q_j(t),\ j = 1, \ldots, N$ and momenta $p_j(t),\ j = 1, \ldots, N$ are solutions of Hamilton's equations:

$$\frac{dq_j(t)}{dt} = \frac{\partial H}{\partial p_j(t)}, \quad \frac{dp_j(t)}{dt} = -\frac{\partial H}{\partial q_j(t)},\ j = 1, \ldots, N. \tag{2}$$

which are 2N first order ODEs which describe the orbits of the system in the 2N–dimensional phase space. If these equations are integrable (a very special situation) the motion is always ordered, while in the generic non–integrable case there are chaotic orbits.

The first example we treat here is the famous FPU 1–dimensional lattice described by the Hamiltonian

$$H = \frac{1}{2}\sum_{j=1}^{N} \dot{x}_j^2 + \sum_{j=0}^{N}\left(\frac{1}{2}(x_{j+1}-x_j)^2 + \frac{1}{4}\beta(x_{j+1}-x_j)^4\right) = E \tag{3}$$

where $q_j = x_j, p_j = \dot{x}_j$.

We then study a lattice with on site potential and **no linear** dispersion, as the coupling between nearest neighbors is of quartic type:

$$H_{NLD} = \frac{1}{2}\sum_{i=1}^{N} p_i^2 + \sum_{i=1}^{N}\left[\frac{1}{2}(q_{i+1}-q_i)^4 + \frac{1}{2}q_i^2(1-\epsilon cos(\omega_d t)) - \frac{1}{4}q_i^4\right] \tag{4}$$

near parameter values where the Hamiltonian has a stable **discrete breather**, under fixed boundary conditions, i.e. $q_0 = q_N = p_0 = p_N = 0$.

Finally, we investigate the dynamics near FPU -like recurrences and stable localized oscillations in chains of coupled symplectic maps of the form:

$$\begin{aligned} x_{n+1}^j &= x_n^j + y_{n+1}^j, \\ y_{n+1}^j &= y_n^j + \frac{K_j}{2\pi}\sin(2\pi x_n^j) - \frac{\beta}{2\pi}\{\sin[2\pi(x_n^{j+1} - x_n^j)] + \sin[2\pi(x_n^{j-1} - x_n^j)]\} \end{aligned} \tag{5}$$

with $j = 1, ..., N$ and $x_0 = x_{N+1} = y_0 = y_{N+1} = 0$. Here, x_n^j are angles and y_n^j are action variables, while "time" ($n = 0, 1, 2, ...$) is discrete. The coupling between nearest neighbors is linearly dispersive and each "particle" in the uncoupled ($\beta = 0$) case is represented by a standard map, which is analogous to a 1-degree of freedom Hamiltonian oscillator.

Geometric Interpretation of the SALI

We note that the SALI may be equivalently evaluated using the 'wedge' product of the two **deviation unit vectors** $\hat{w}_1 \wedge \hat{w}_1$ for which it holds

$$\|\hat{w}_1 \wedge \hat{w}_2\| = \frac{\|\hat{w}_1 - \hat{w}_2\| \cdot \|\hat{w}_1 + \hat{w}_2\|}{2} \quad . \tag{6}$$

Thus, the SALI is related to **the 'area' between the 2 deviation vectors**, $\hat{w}_1$, $\hat{w}_2$.
Generalizing to more than two deviations $\hat{w}_1, \hat{w}_2, \ldots, \hat{w}_k$, $2 \leq k \leq 2N$, we introduce an index that is proportional to **the 'volume' of the parallelepiped** that has these vectors as vertices.
All normalized deviation vectors $\hat{w}_i$, $i = 1, 2, \ldots, 2N$, can be written as

$$\hat{w}_i = \sum_{j=1}^{2N} w_{ij} \hat{e}_j \quad , \quad i = 1, 2, \ldots, k \tag{7}$$

when expressed in terms of the usual orthonormal basis of the n–dimensional Euclidean space.

The wedge product of these k deviation vectors can be written with respect to the basis $\hat{e}_{i_k}$

$$\hat{w}_1 \wedge \hat{w}_2 \wedge \cdots \wedge \hat{w}_k = \sum_{1 \le i_1 < i_2 < \cdots < i_k \le 2N} \begin{vmatrix} w_{1i_1} & w_{1i_2} & \cdots & w_{1i_k} \\ w_{2i_1} & w_{2i_2} & \cdots & w_{2i_k} \\ \vdots & \vdots & & \vdots \\ w_{ki_1} & w_{ki_2} & \cdots & w_{ki_k} \end{vmatrix} \hat{e}_{i_1} \wedge \hat{e}_{i_2} \wedge \cdots \wedge \hat{e}_{i_k} \quad (8)$$

If **at least two** of the normalized deviation vectors $\hat{w}_i$, $i = 1, 2, \ldots, k$ are **linearly dependent**, all the $k \times k$ determinants will become zero **making the 'volume' vanish**. We define the norm of this quantity, as the **Generalized ALignment Index**

$$GALI_k(t) = \|\hat{w}_1(t) \wedge \hat{w}_2(t) \wedge \cdots \wedge \hat{w}_k(t)\|,$$

or

$$GALI_k(t) = \left\{ \sum_{1 \le i_1 < i_2 < \cdots < i_k \le 2N} \begin{vmatrix} w_{1i_1} & w_{1i_2} & \cdots & w_{1i_k} \\ w_{2i_1} & w_{2i_2} & \cdots & w_{2i_k} \\ \vdots & \vdots & & \vdots \\ w_{ki_1} & w_{ki_2} & \cdots & w_{ki_k} \end{vmatrix}^2 \right\}^{1/2} \quad (9)$$

Exponential decay of GALI for chaotic orbits

Let us first investigate the dynamics in the vicinity of a chaotic orbit of the Hamiltonian system, with N degrees of freedom. Let $L_1 \geq L_2 \geq \cdots \geq L_{2N}$ be the 'local Lyapunov exponents' oscillating about their time averaged values

$$\sigma_1 \geq \sigma_2 \geq \cdots \geq \sigma_{N-1} \geq \sigma_N = \sigma_{N+1} = 0 \geq \sigma_{N+2} \geq \cdots \geq \sigma_{2N}. \tag{10}$$

which are the 'global' LCEs. Assuming that the L_i, $i = 1, 2, \ldots, 2N$ do not fluctuate significatively, the evolution of any initial deviation vector $\vec{w}_i$ may be written as

$$\vec{w}_i(t) = \sum_{j=1}^{2N} c_j^i \, e^{\sigma_j t} \, \hat{u}_j \, , \tag{11}$$

A leading order estimate of the deviation vector's Euclidean norm, for long enough times, is

$$\|\vec{w}_i(t)\| \approx |c_1^i| e^{\sigma_1 t} \, . \tag{12}$$

The determinants appearing in the definition of $GALI_k$ (see equation (9)) can be divided in two categories depending on whether or not they contain the first column of the corresponding matrix. Those that **do contain the first column** yield ($s_i = \pm 1$)

$$D_{1,j_1,j_2,\ldots,j_{k-1}} = \begin{vmatrix} s_1 & \frac{c^1_{j_1}}{|c^1_1|} e^{-(\sigma_1-\sigma_{j_1})t} & \cdots & \frac{c^1_{j_{k-1}}}{|c^1_1|} e^{-(\sigma_1-\sigma_{j_{k-1}})t} \\ s_2 & \frac{c^2_{j_1}}{|c^2_1|} e^{-(\sigma_1-\sigma_{j_1})t} & \cdots & \frac{c^2_{j_{k-1}}}{|c^2_1|} e^{-(\sigma_1-\sigma_{j_{k-1}})t} \\ \vdots & \vdots & & \vdots \\ s_k & \frac{c^k_{j_1}}{|c^k_1|} e^{-(\sigma_1-\sigma_{j_1})t} & \cdots & \frac{c^k_{j_{k-1}}}{|c^k_1|} e^{-(\sigma_1-\sigma_{j_{k-1}})t} \end{vmatrix} =$$

$$= \begin{vmatrix} s_1 & \frac{c^1_{j_1}}{|c^1_1|} & \cdots & \frac{c^1_{j_{k-1}}}{|c^1_1|} \\ s_2 & \frac{c^2_{j_1}}{|c^2_1|} & \cdots & \frac{c^2_{j_{k-1}}}{|c^2_1|} \\ \vdots & \vdots & & \vdots \\ s_k & \frac{c^k_{j_1}}{|c^k_1|} & \cdots & \frac{c^k_{j_{k-1}}}{|c^k_1|}. \end{vmatrix} e^{-\left[(\sigma_1-\sigma_{j_1})+(\sigma_1-\sigma_{j_2})+\cdots+(\sigma_1-\sigma_{j_{k-1}})\right]t} \qquad (13)$$

Thus, the time evolution of $D_{1,j_1,j_2,\ldots,j_{k-1}}$ is mainly determined by the exponential law

$$D_{1,j_1,j_2,\ldots,j_{k-1}} \propto e^{-\left[(\sigma_1-\sigma_{j_1})+(\sigma_1-\sigma_{j_2})+\cdots+(\sigma_1-\sigma_{j_{k-1}})\right]t} . \quad (14)$$

The determinants that **do not contain the first column** of the transformation matrix tend to zero following an exponential law that decays faster.

Clearly, from all determinants the one that decreases the *slowest* is the one containing the first k columns of the transformation matrix, yielding the approximation that GALI$_k$ tends to zero as

$$\text{GALI}_k(t) \propto e^{-[(\sigma_1-\sigma_2)+(\sigma_1-\sigma_3)+\cdots+(\sigma_1-\sigma_k)]t} . \quad (15)$$

The evaluation of GALI for ordered orbits

As is well–known, ordered orbits typically lie on N–dimensional tori, which can be described by a local transformation to action–angle variables, locally satisfying

$$\begin{aligned} \dot{J}_i &= 0 \\ \dot{\theta}_i &= \omega_i(J_1, J_2, \ldots, J_N) \end{aligned} \qquad i = 1, 2, \ldots, N. \tag{16}$$

These can be easily integrated to give

$$\begin{aligned} J_i(t) &= J_{i0} \\ \theta_i(t) &= \theta_{i0} + \omega_i(J_{10}, J_{20}, \ldots, J_{N0})\, t \end{aligned} \qquad i = 1, 2, \ldots, N, \tag{17}$$

By denoting as ξ_i, η_i, $i = 1, 2, \ldots, N$ small deviations of J_i and θ_i respectively, the variational equations of system (16), can be solved to yield:

$$\begin{aligned} \xi_i(t) &= \xi_i(0) \\ \eta_i(t) &= \eta_i(0) + \left[\sum_{j=1}^{N} \omega_{ij}\xi_j(0)\right]\, t \end{aligned} \qquad i = 1, 2, \ldots, N. \tag{18}$$

This implies a linear increase of the norm of the deviation vector

$$\|\vec{w}(t)\| = \left\{ 1 + \left[\sum_{i=1}^{N} \left(\sum_{j=1}^{N} \omega_{ij} \xi_j(0) \right) \right] t^2 + \left[2 \sum_{i=1}^{N} \left(\eta_i(0) \sum_{j=1}^{N} \omega_{ij} \xi_j(0) \right) \right] t \right\}^{1/2}, \quad (19)$$

Therefore, the normalized deviation vector tends to **fall on the tangent space of the torus**, since its coordinates **along the action directions vanish** following a t^{-1} rate.
Let us now study the general case of k, linearly independent unit deviation vectors $\{\hat{w}_1, \hat{w}_2, \ldots, \hat{w}_k\}$ with $2 \leq k \leq 2N$. Using as vector basis the set $\{\hat{v}_1, \hat{v}_2, \ldots, \hat{v}_{2N}\}$ we get:

$$\left[\begin{array}{cccc} \hat{w}_1 & \hat{w}_2 & \ldots & \hat{w}_k \end{array} \right]^{\mathrm{T}} = \mathbf{D} \cdot \left[\begin{array}{cccc} \hat{v}_1 & \hat{v}_2 & \ldots & \hat{v}_{2N} \end{array} \right]^{\mathrm{T}} \quad (20)$$

If *no* deviation vector is initially located in the tangent space of the torus, matrix **D** has the form

$$\mathbf{D} = [d_{ij}] = \frac{1}{\prod_{m=1}^{k} \|\vec{w}_m(t)\|} \cdot \mathbf{D}^k(t). \quad (21)$$

where $i = 1, 2, \ldots, k$ and $j = 1, 2, \ldots, 2N$. Recalling our earlier discussion, the norm of vector $\vec{w}_i(t)$ for long times, grows linearly with t as

$$M_i(t) = \|\vec{w}_i(t)\| \propto t. \tag{22}$$

the matrix **D** assumes the much simpler form

$$\mathbf{D}(t) = \frac{1}{t^k} \cdot \mathbf{D}^k(t). \tag{23}$$

The Case of N-Dimensional Tori

If k is lower than the dimension of the tangent space of the torus, i. e. $2 \leq k \leq N$, the fastest increasing determinants in this case are $\propto t^k$. Thus, we conclude that the contribution to the behavior of $GALI_k$ is to provide constant terms.
All other determinants introduce terms that grow at a rate **slower** than t^k, proportional to $t^{k-m}/t^k = 1/t^m$. So we arrive at the important result

$$\text{GALI}_k(t) \approx \text{constant} \;\; \text{for} \;\; 2 \leq k \leq N. \tag{24}$$

In the important case of $N < k \leq 2N$ deviation vectors, the fastest growing determinants have the time evolution

$$Determinants \propto t^{2N-k}. \tag{25}$$

and contribute to the time evolution of $GALI_k$ terms proportional to

$$\text{GALI}_k(t) \propto t^{2N-k}/t^k = 1/t^{2(k-N)}. \tag{26}$$

All other determinants introduce terms that tend to zero faster than $1/t^{2(k-N)}$.

The Case of Tori with Dimension Lower than N

In the case of an s–dimensional torus, the k deviation vectors eventually fall on its s–dimensional tangent space spanned by $\hat{v}_{N+1}, \ldots, \hat{v}_{N+s}$. If we start with $2 \leq k \leq s$ deviation vectors, the GALI$_k$ indices will oscillate about **a nonzero constant**. However, for $s < k \leq 2N$ deviation vectors, some of them will become linearly dependent and the GALI$_k$ will **tend to zero by a power law**.

Let us first turn to the case of $s < k \leq 2N - s$. The fastest growing determinants are those containing the s columns of the matrix $\mathbf{D}^k$ with $\omega_{ij} \neq 0$, having as many columns proportional to t as possible. Since t appears at most s times and GALI$_k$ is proportional to $t^s/t^k = 1/t^{(k-s)}$, we conclude that GALI$_k(t) \sim t^{(s-k)}$ for $s < k \leq 2N - s$.
Finally, we consider the behavior of GALI$_k$ when $2N - s < k \leq 2N$. The fastest growing determinants here have t appearing $2N - k$ times and the GALI$_k$ is proportional to $t^{2N-k}/t^k = 1/t^{2(k-N)}$.
In conclusion, we have shown that for chaotic orbits:

$$\text{GALI}_k(t) \propto e^{-[(\sigma_1-\sigma_2)+(\sigma_1-\sigma_3)+\cdots+(\sigma_1-\sigma_k)]t} . \tag{27}$$

while for regular orbits lying on an s–dimensional torus behave as:

$$\text{GALI}_k(t) \sim \begin{cases} \text{constant} & \text{if } 2 \leq k \leq s \\ \frac{1}{t^{k-s}} & \text{if } s < k \leq 2N - s \\ \frac{1}{t^{2(k-N)}} & \text{if } 2N - s < k \leq 2N \end{cases} . \tag{28}$$

Note that from (28) we deduce that for $s = N$, GALI$_k$ remains constant for $2 \leq k \leq N$ and decreases to zero as $\sim 1/t^{2(k-N)}$ for $N < k \leq 2N$.

GALI$_k(t)$: Numerical Computations and the SVD Approach

We can write equations (7) in matrix form as:

$$\begin{bmatrix} \hat{w}_1 \\ \hat{w}_2 \\ \vdots \\ \hat{w}_k \end{bmatrix} = \begin{bmatrix} w_{11} & w_{12} & \cdots & w_{1\,2N} \\ w_{21} & w_{22} & \cdots & w_{2\,2N} \\ \vdots & \vdots & & \vdots \\ w_{k1} & w_{k2} & \cdots & w_{k\,2N} \end{bmatrix} \cdot \begin{bmatrix} \hat{e}_1 \\ \hat{e}_2 \\ \vdots \\ \hat{e}_{2N} \end{bmatrix} = \mathbf{A} \cdot \begin{bmatrix} \hat{e}_1 \\ \hat{e}_2 \\ \vdots \\ \hat{e}_{2N} \end{bmatrix} . \qquad (29)$$

Since GALI$_k$ measures the volume of the k–parallelepiped P_k having as edges the k unitary deviation vectors $\hat{w}_i$, $i = 1, \ldots, k$, given by:

$$\text{vol}(P_k) = \sqrt{\det(\mathbf{A} \cdot \mathbf{A}^{\mathrm{T}})} \ , \qquad (30)$$

(where $(^{\mathrm{T}})$ denotes transpose), we finally have:

$$\text{GALI}_k = \sqrt{\det(\mathbf{A} \cdot \mathbf{A}^{\mathrm{T}})}, \qquad (31)$$

where only the multiplication of two matrices and the square root of one determinant appears.

Thus we can avoid the computation of many determinants and evaluate GALI$_k$ by performing the Singular Value Decomposition (SVD) of $\mathbf{A}^{\mathrm{T}}$ as follows: The $2N \times k$ matrix $\mathbf{A}^{\mathrm{T}}$ is written as the product of a $2N \times k$ column–orthogonal matrix **U**, a $k \times k$ diagonal matrix **Z** with elements z_i, $i = 1, \ldots, k$ (the so–called *singular values*), and the transpose of a $k \times k$ orthogonal matrix **V**:

$$\mathbf{A}^{\mathrm{T}} = \mathbf{U} \cdot \mathbf{Z} \cdot \mathbf{V}^{\mathrm{T}}. \tag{32}$$

We note that matrices **U** and **V** are orthogonal so that:

$$\mathbf{U}^{\mathrm{T}} \cdot \mathbf{U} = \mathbf{V}^{\mathrm{T}} \cdot \mathbf{V} = \mathrm{I}_k, \tag{33}$$

I_k being the $k \times k$ unit matrix. Using Eq. (31) for the computation of GALI$_k$, as well as Eqs. (32) and (33), we get:

$$\begin{aligned} \mathrm{GALI}_k &= \sqrt{\det\left(\mathbf{A} \cdot \mathbf{A}^{\mathrm{T}}\right)} = \sqrt{\det\left(\mathbf{V} \cdot \mathbf{Z}^{\mathrm{T}} \cdot \mathbf{U}^{\mathrm{T}} \cdot \mathbf{U} \cdot \mathbf{Z} \cdot \mathbf{V}^{\mathrm{T}}\right)} \\ &= \sqrt{\det\left(\mathbf{V} \cdot \mathrm{diag}(z_i^2) \cdot \mathbf{V}^{\mathrm{T}}\right)} = \sqrt{\det\left(\mathrm{diag}(z_i^2)\right)} = \prod_{i=1}^{k} z_i \, . \end{aligned}$$

Applications of GALI for Detecting Chaos and Order

We shall use two examples with 2 (2D) and 3 (3D) degrees of freedom: the 2D Hénon–Heiles Hamiltonian

$$H_2 = \frac{1}{2}(p_x^2 + p_y^2) + \frac{1}{2}(x^2 + y^2) + x^2 y - \frac{1}{3}y^3, \tag{34}$$

and the 3D Hamiltonian system:

$$H_3 = \sum_{i=1}^{3} \frac{\omega_i}{2}(q_i^2 + p_i^2) + q_1^2 q_2 + q_1^2 q_3, \tag{35}$$

for the parameters $H_2 = 0.125$ and $H_3 = 0.09$, with $\omega_1 = 1$, $\omega_2 = \sqrt{2}$ and $\omega_3 = \sqrt{3}$.

A 2D Hamiltonian system

Let us consider first a chaotic orbit of the 2D Hamiltonian (34), with initial conditions $x = 0$, $y = -0.25$, $p_x = 0.42$, $p_y = 0$. In the figure below, we see the time evolution of $L_1(t)$ of this orbit, which is a good approximation of the maximal LCE, σ_1. Actually, for $t \approx 10^5$, we find $\sigma_1 \approx 0.047$.

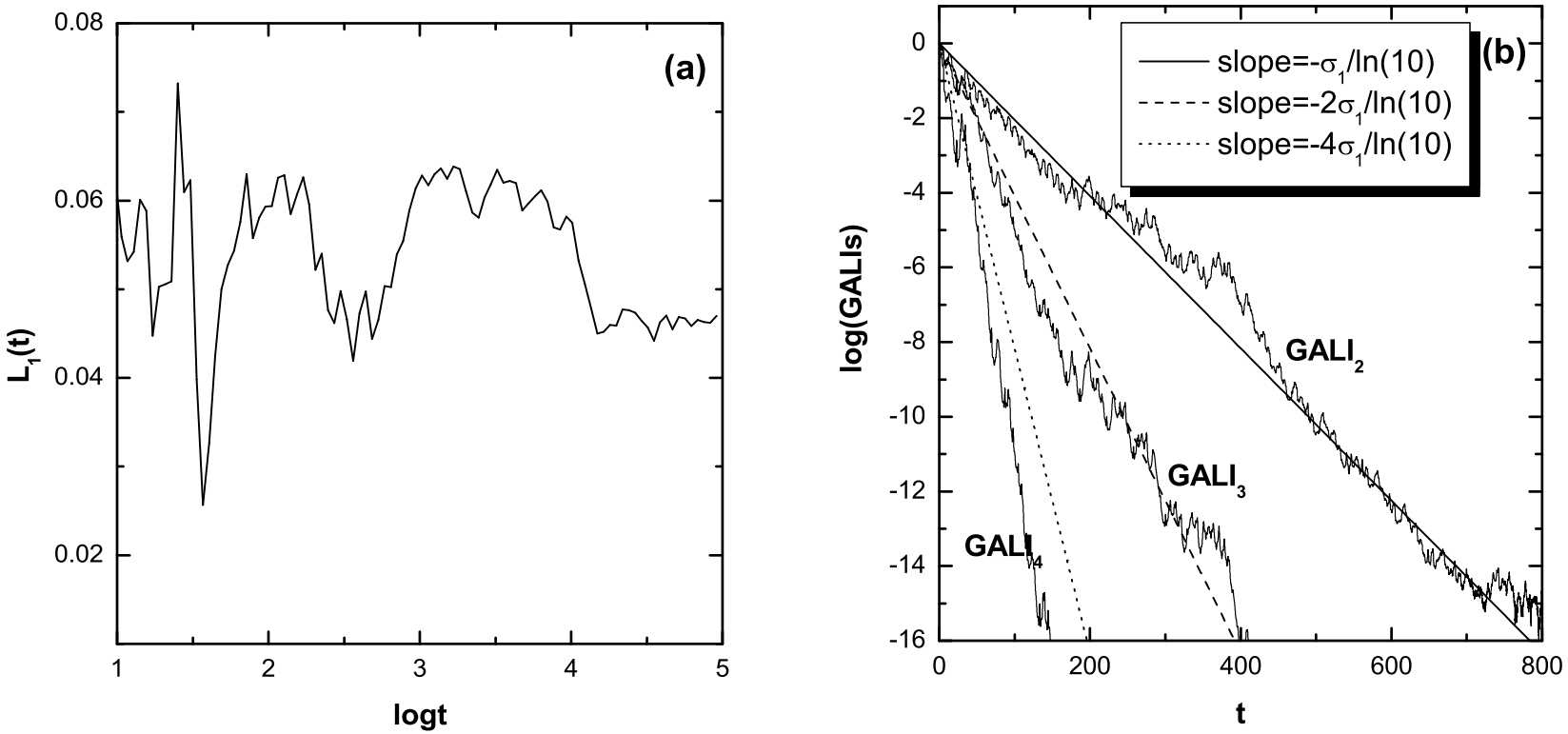

Figure 11:(a) $L_1(t)$ for a chaotic orbit of the 2D system. (b) The evolution of GALI$_2$, GALI$_3$ and GALI$_4$ for the same orbit. We find $\sigma_1 \approx 0.047$, and we know $\sigma_2 = 0$ and $\sigma_3 = -\sigma_2$ and $\sigma_4 = -\sigma_1$. So, GALI$_k$ behaves as

$$\text{GALI}_2(t) \propto e^{-\sigma_1 t}, \;\; \text{GALI}_3(t) \propto e^{-2\sigma_1 t}, \;\; \text{GALI}_4(t) \propto e^{-4\sigma_1 t}. \qquad (36)$$

A 3D Hamiltonian system

Let us now study the behavior of the GALIs in the case of the 3D Hamiltonian (35). The initial conditions of the orbits of this system are defined by assigning arbitrary values to the positions q_1, q_2, q_3, as well as the so–called 'harmonic energies' E_1, E_2, E_3 related to the momenta through $p_i = \sqrt{\frac{2E_i}{\omega_i}}$, $i = 1, 2, 3$.

Chaotic orbits of 3D Hamiltonian systems generally have two positive Lyapunov exponents, σ_1 and σ_2, while $\sigma_3 = 0$. So, for approximating the behavior of GALIs according to (47), both σ_1 and σ_2 are needed. In particular, (47) gives

$$\begin{gathered} \text{GALI}_2(t) \propto e^{-(\sigma_1-\sigma_2)t}, \;\; \text{GALI}_3(t) \propto e^{-(2\sigma_1-\sigma_2)t}, \;\; \text{GALI}_4(t) \propto e^{-(3\sigma_1-\sigma_2)t}, \\ \text{GALI}_5(t) \propto e^{-4\sigma_1 t}, \;\; \text{GALI}_6(t) \propto e^{-6\sigma_1 t}. \end{gathered} \tag{37}$$

Let us consider the chaotic orbit with initial conditions $q_1 = q_2 = q_3 = 0$, $E_1 = E_2 = E_3 = 0.03$ of the 3D system (35) and compute σ_1, σ_2 for this orbit. For $t \approx 10^5$ we find $\sigma_1 \approx 0.03$ and $\sigma_2 \approx 0.008$. Using these values as good approximations of σ_1, σ_2 we see that the slopes of all GALIs are well reproduced by the analytical formulas.

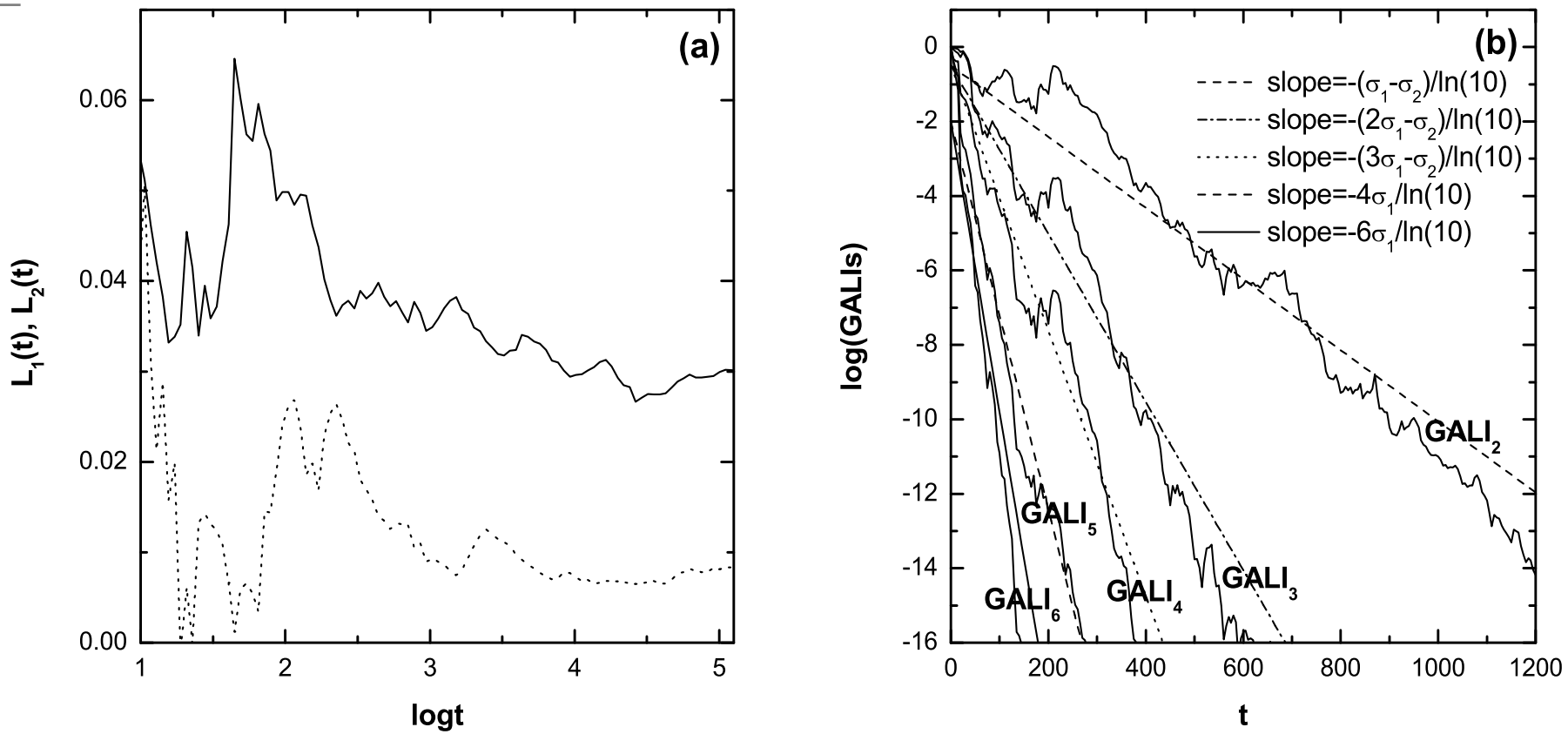

Figure 12: (a) The evolution of $L_1(t)$, $L_2(t)$ for the chaotic orbit of the 3D system. (b) The evolution of GALI$_k$ with $k = 2, \ldots, 6$. The plotted lines correspond to functions proportional to $e^{-(\sigma_1-\sigma_2)t}$, $e^{-(2\sigma_1-\sigma_2)t}$, $e^{-(3\sigma_1-\sigma_2)t}$, $e^{-4\sigma_1 t}$ and $e^{-6\sigma_1 t}$ for $\sigma_1 = 0.03$, $\sigma_2 = 0.008$.

Next, we consider the case of ordered orbits in our 3D Hamiltonian system. In general, the GALIs should behave as: $\text{GALI}_2(t) \propto$ constant, $\text{GALI}_3(t) \propto$ constant, $\text{GALI}_4(t) \propto \frac{1}{t^2}$, $\text{GALI}_5(t) \propto \frac{1}{t^4}$, $\text{GALI}_6(t) \propto \frac{1}{t^6}$.

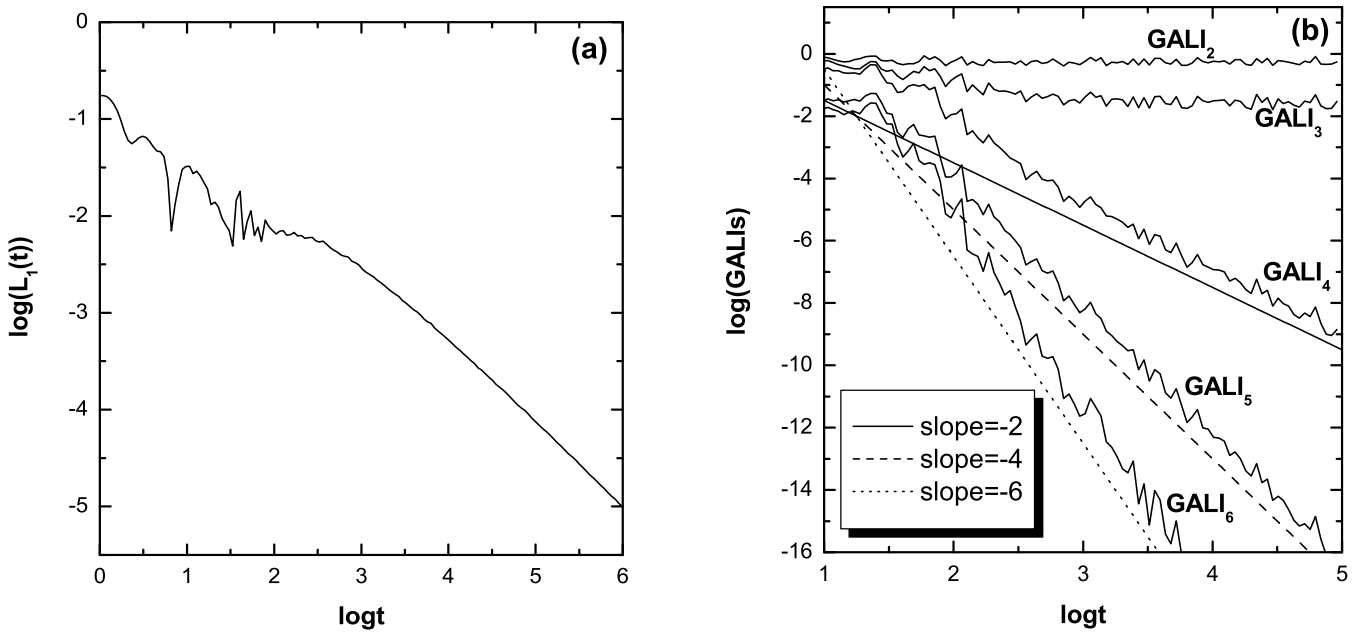

Figure 13: (a) $L_1(t)$ for the ordered orbit of the 3D system and (b) The GALI_k with $k = 2, \ldots, 6$ of the same orbit. The dashed lines are the slopes of $\frac{1}{t^2}$, $\frac{1}{t^4}$ and $\frac{1}{t^6}$.

Dimensionality of Tori and Diffusion in FPU Lattices

In their famous paper in 1955, Fermi, Pasta and Ulam studied energy transport in one – dimensional lattices, like the so – called β – FPU lattice described by the Hamiltonian

$$H = \frac{1}{2}\sum_{j=1}^{N}\dot{x}_j^2 + \sum_{j=0}^{N}\left(\frac{1}{2}(x_{j+1}-x_j)^2 + \frac{1}{4}\beta(x_{j+1}-x_j)^4\right) = E \tag{38}$$

When β is small, the dynamics can described by the linear normal modes

$$Q_k = \sqrt{\frac{2}{N+1}}\sum_{i=1}^{N} q_i \sin\frac{ki\pi}{N+1}, \qquad P_k = \dot{Q}_k \tag{39}$$

with energies and ("phonon") frequencies

$$E_k = \frac{1}{2}\left[P_k^2 + {\omega_k}^2 Q_k^2\right], \;\; \omega_k = 2\sin\frac{k\pi}{2(N+1)} \tag{40}$$

Fermi, Pasta and Ulam observed that, for low values of E, if the initial conditions are chosen such that one or more of the **low k - modes** ($k = 1, 2, 3, ..$) are excited, one observes the famous **FPU recurrences**!

This means that the energy returns periodically to the initial state, instead of leading to energy sharing and equipartition as expected from Statistical Mechanics. Let us see what the GALI$_k$ give when only the $k = 1$ and $k = 3$ modes modes are excited:

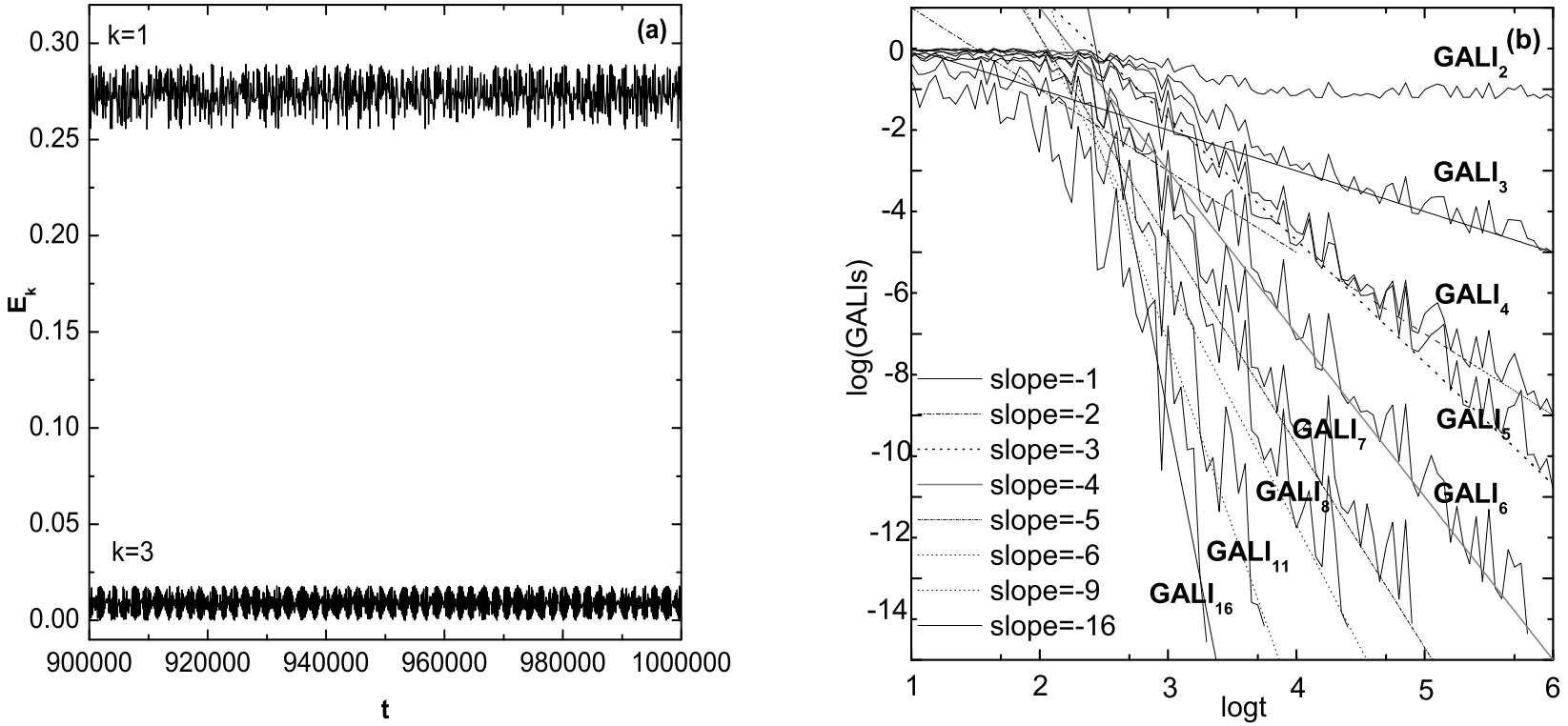

Figure 14: FPU with 8 particles:(a) Only the E_1 and E_3 modes are excited and the torus is 2-dimensional, since (b) only GALI$_2$=const. and all other GALI$_k$ decay by the expected power laws.

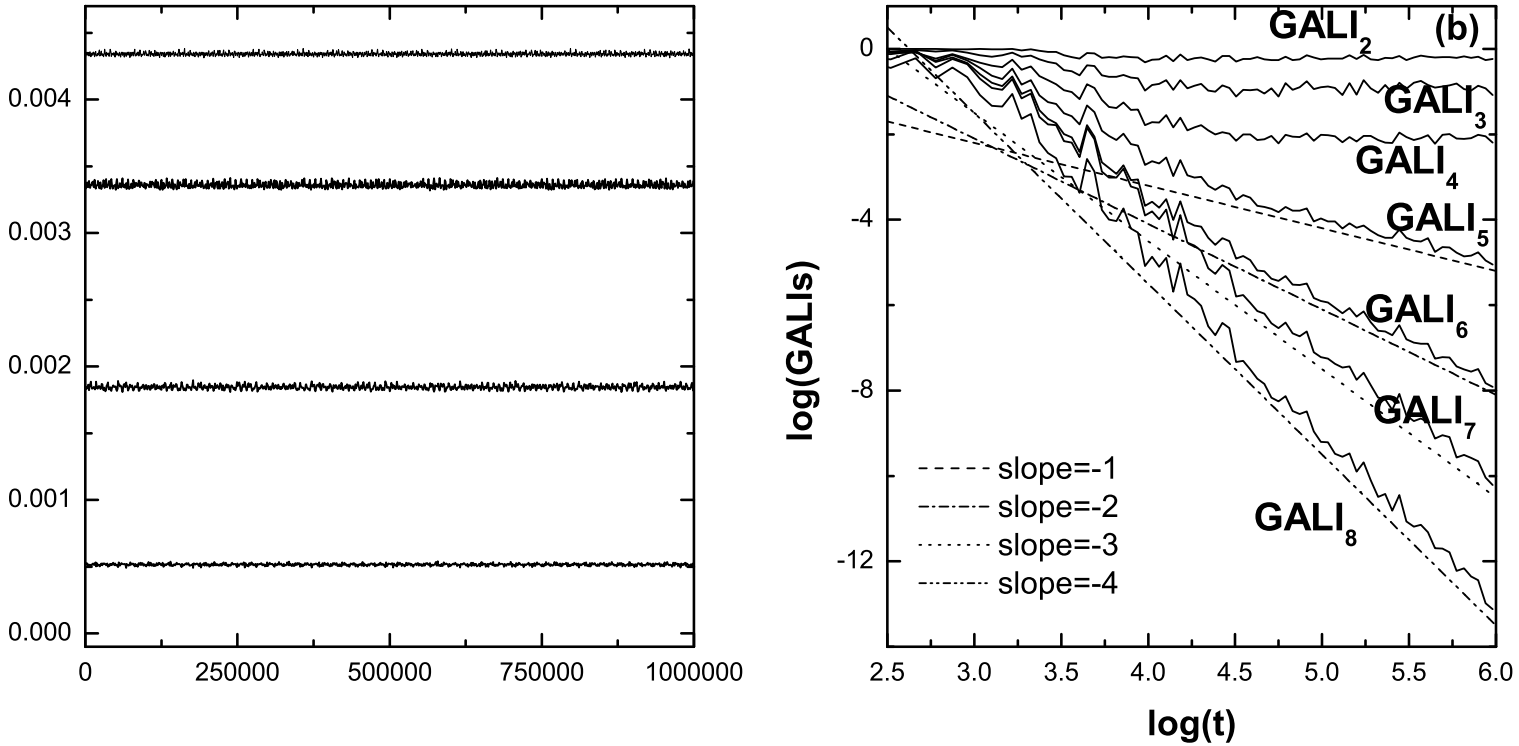

Figure 15 (a) The time evolution of harmonic energies for a regular orbit lying on a 4–dimensional torus of the $N = 8$ particle FPU lattice. Recurrences occur between E_1, E_3, E_5 and E_7, while all other harmonic energies are practically zero. The time evolution of the corresponding GALI$_k$ is plotted in (b) for $k = 2, \ldots, 8$. The plotted lines in (b) correspond to the power laws predicted in (28).

Predicting the onset of weak diffusion

For initial conditions **slightly off a torus** leading to slow diffusive motion away from quasiperiodicity, the GALI$_k$ predicts it quickly by falling to zero **exponentially**:

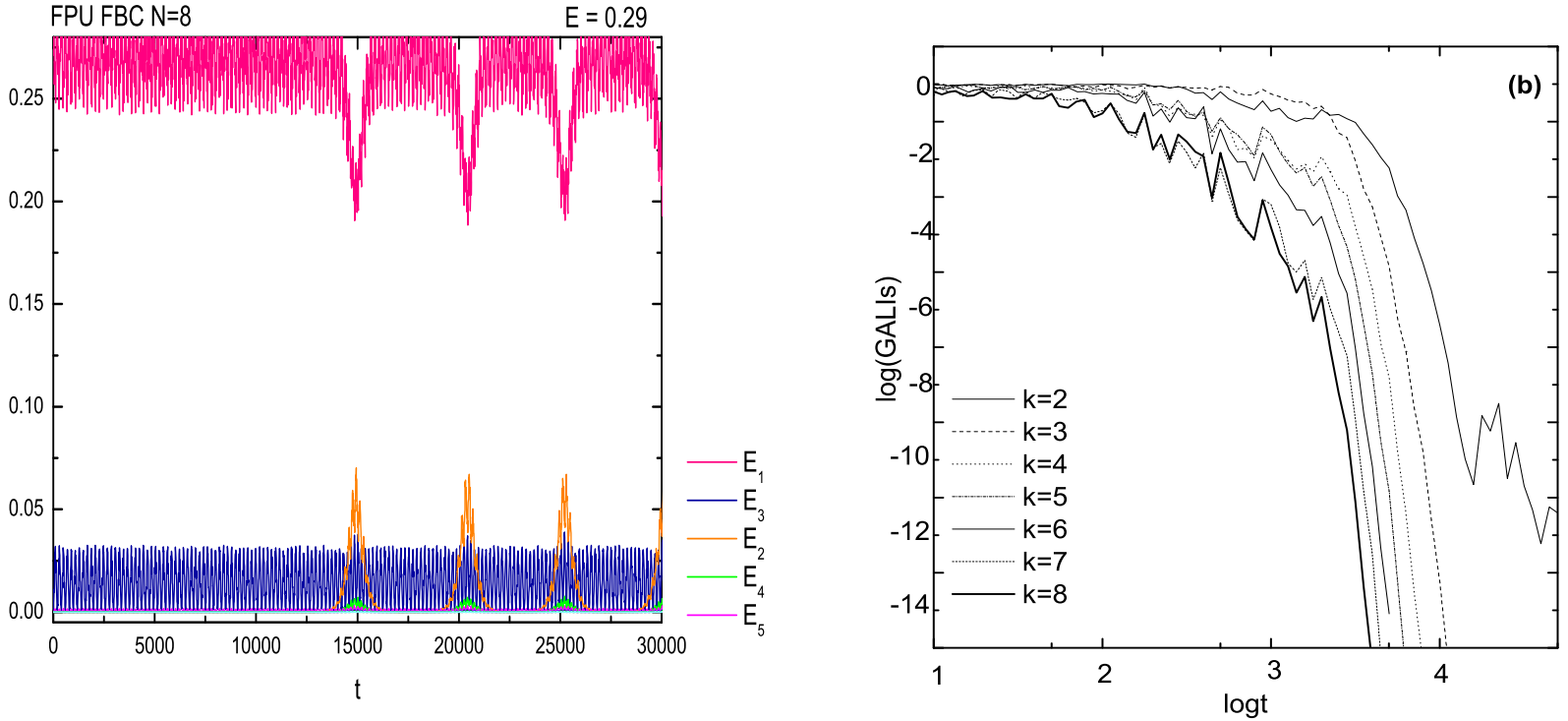

Figure 16: FPU with 8 particles:(a) The evolution of GALI$_2$ shows already at $t \approx 500$ that the orbit diffuses away from the torus and is not quasiperiodic. (b) This becomes visible in the oscillations **much later**, when the recurrences break down at $t \approx 14000$.

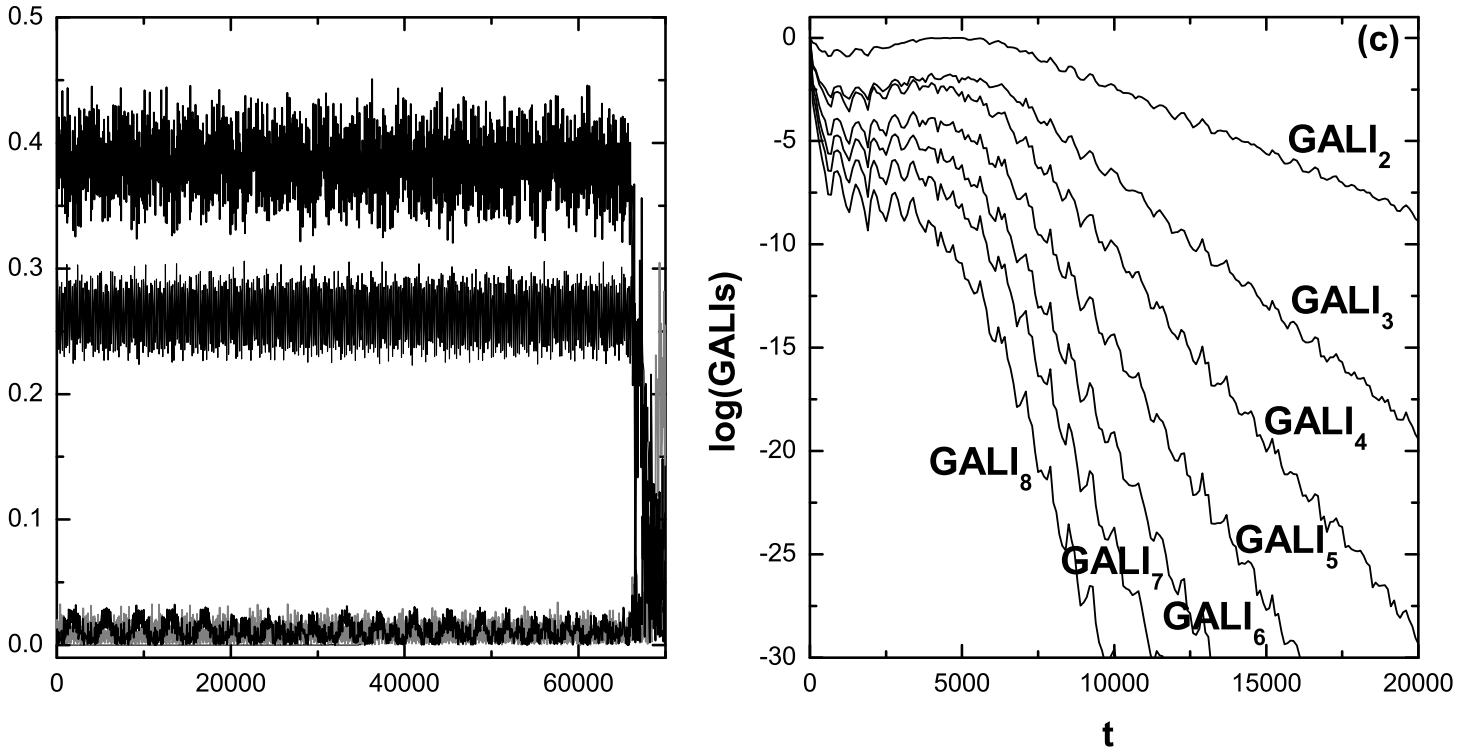

Figure 16 The time evolution of harmonic energies (a) E_1, E_3, E_5, E_7, for a slowly diffusing orbit of the $N = 8$ particle FPU lattice. (b) The time evolution of the corresponding GALI$_k$ for $k = 2, \ldots, 8$, clearly exhibits exponential decay already at $t \approx 10000$.

On the Dynamics Near Stable Discrete Breathers

Quasiperiodic Breathers and their Breakdown

Finally we study a quartic Hamiltonian lattice with on site quartic potential and no linear dispersion, described by the Hamiltonian

$$H_{NL} = \frac{1}{2}\sum_{i=1}^{N} p_i^2 + \sum_{i=1}^{N}\left[\frac{1}{2}(q_{i+1}-q_i)^4 + \frac{1}{2}q_i^2(1-\epsilon cos(\omega_d t)) - \frac{1}{4}q_i^4\right] \quad (41)$$

with fixed boundary conditions, i.e. $q_0 = q_N = p_0 = p_N = 0$. We select parameter values at which we know that the Hamiltonian (41) has a stable **discrete breather**. The particular parameter where this exact breather exists is D=1.2

Now, around this (periodic) breather, due to the **absence of quadratic nearest neighbor interactions**–and hence no linear spectrum to generate resonances–**quasiperiodic breathers** are expected. Indeed, GALI$_2$ oscillates about a constant and thus identifies the presence of a torus. And since **all higher order** GALI$_k$, with $k > 2$, decay the torus is 2–dimensional!

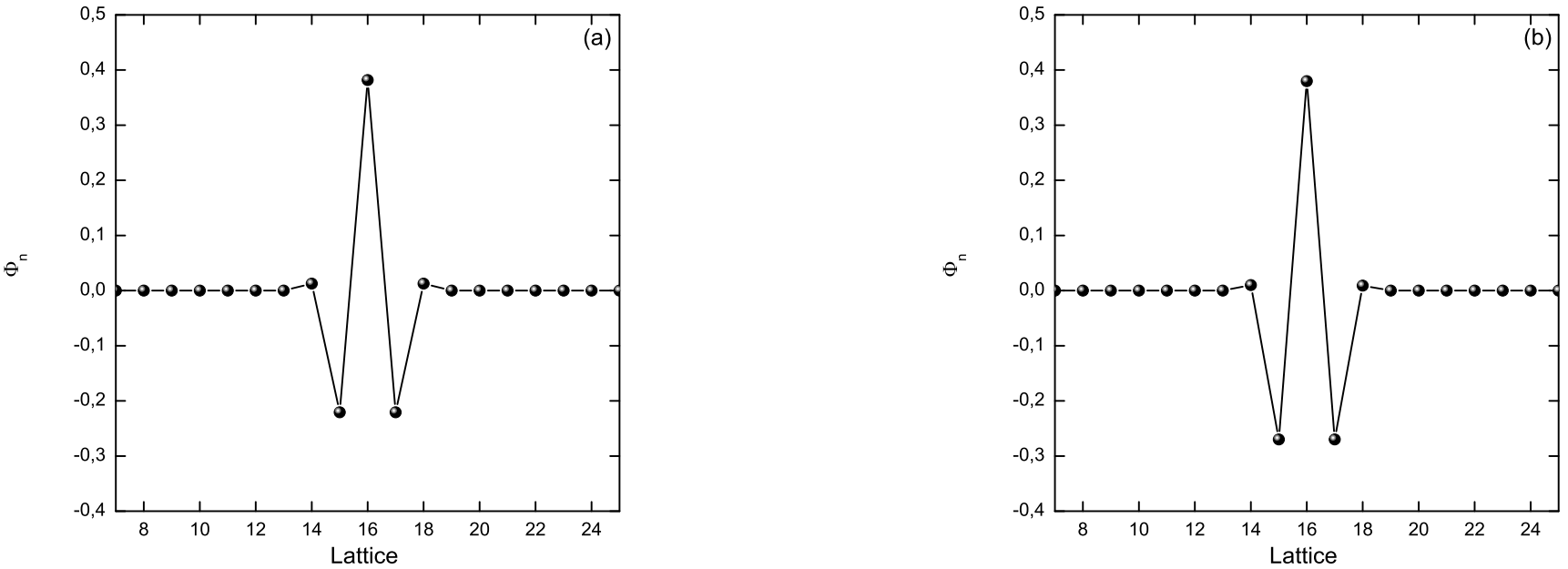

Figure 17: (a) Initial conditions $x_n = D\Phi_n$ for a 31 particle lattice with velocities set to zero, where Φ_n are homoclinic intersections of a cubic map and $D = 1.2$ corresponds to a periodic breather. (b) We perturb the initial conditions by varying $D = 1, 0.9, 0.8$, etc., so that the amplitudes of the central particles slightly change.

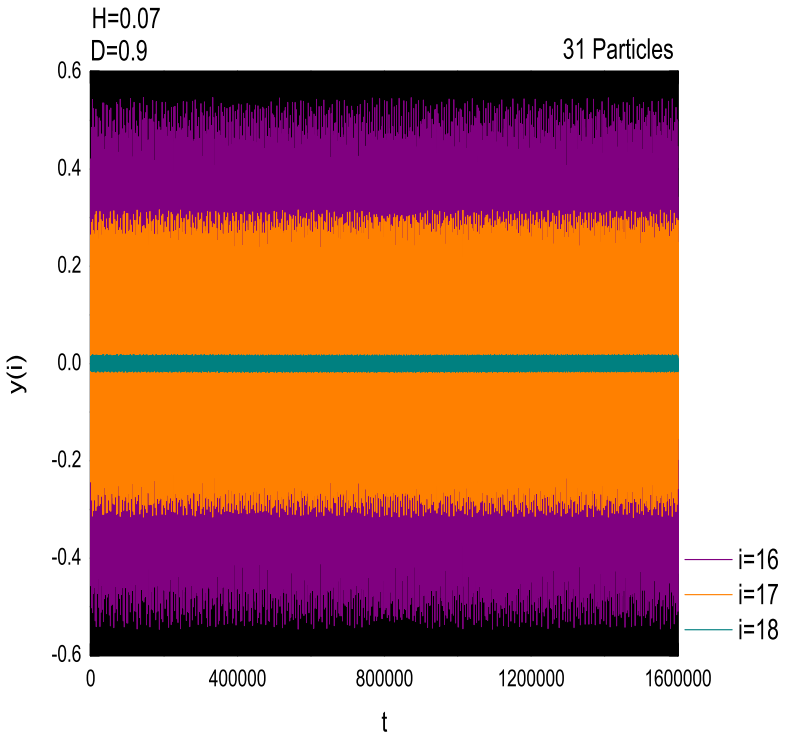

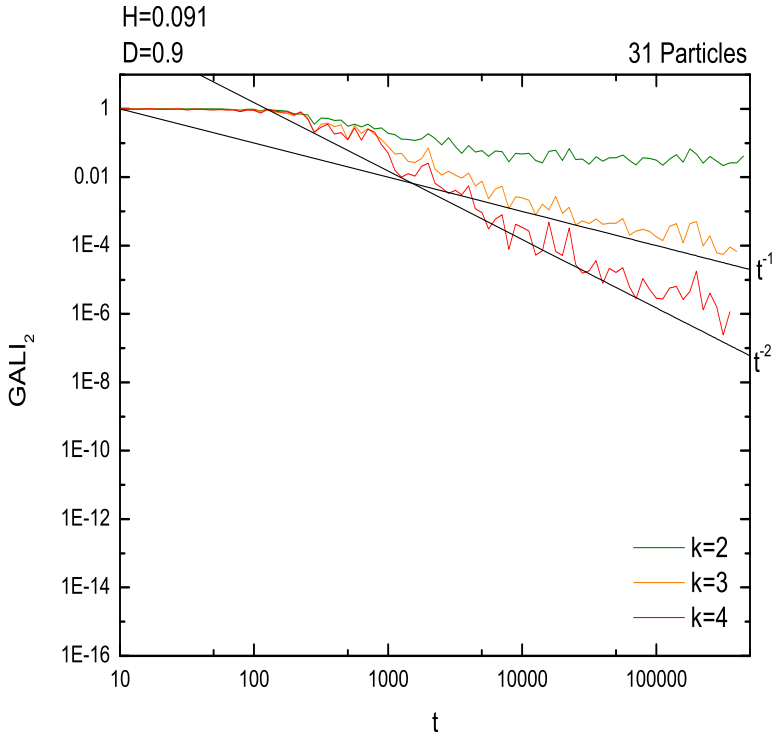

Figure 18:(a) At D=0.9, the oscillations of the central three particles of this $N = 31$ lattice do **not break down**, forming a quasiperiodic breather. (b) The corresponding torus, at this energy, is 2–dimensional, since only GALI_2 remains nearly constant, while all other GALI_k, with $k > 2$ decay by power laws.

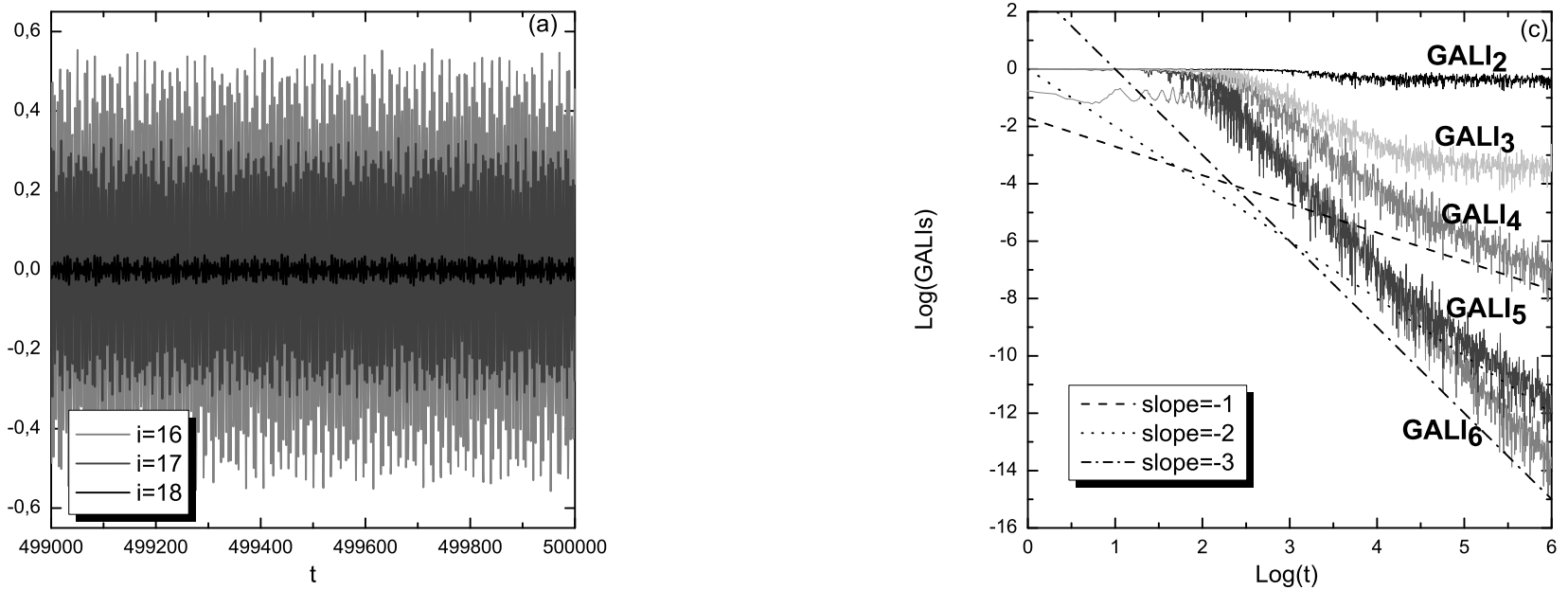

Figure 19: (a) Oscillations of particles 16, 17, 18 in the 31 particle lattice. (b) Time evolution of GALI$_k$ indices for $D = 0.8$ and $H_0 = 0.062$. The breather remains quasiperiodic for very long times, lying on a 3–dimensional torus. Again the slopes of GALI$_k$ indices coincide with the theoretical laws.

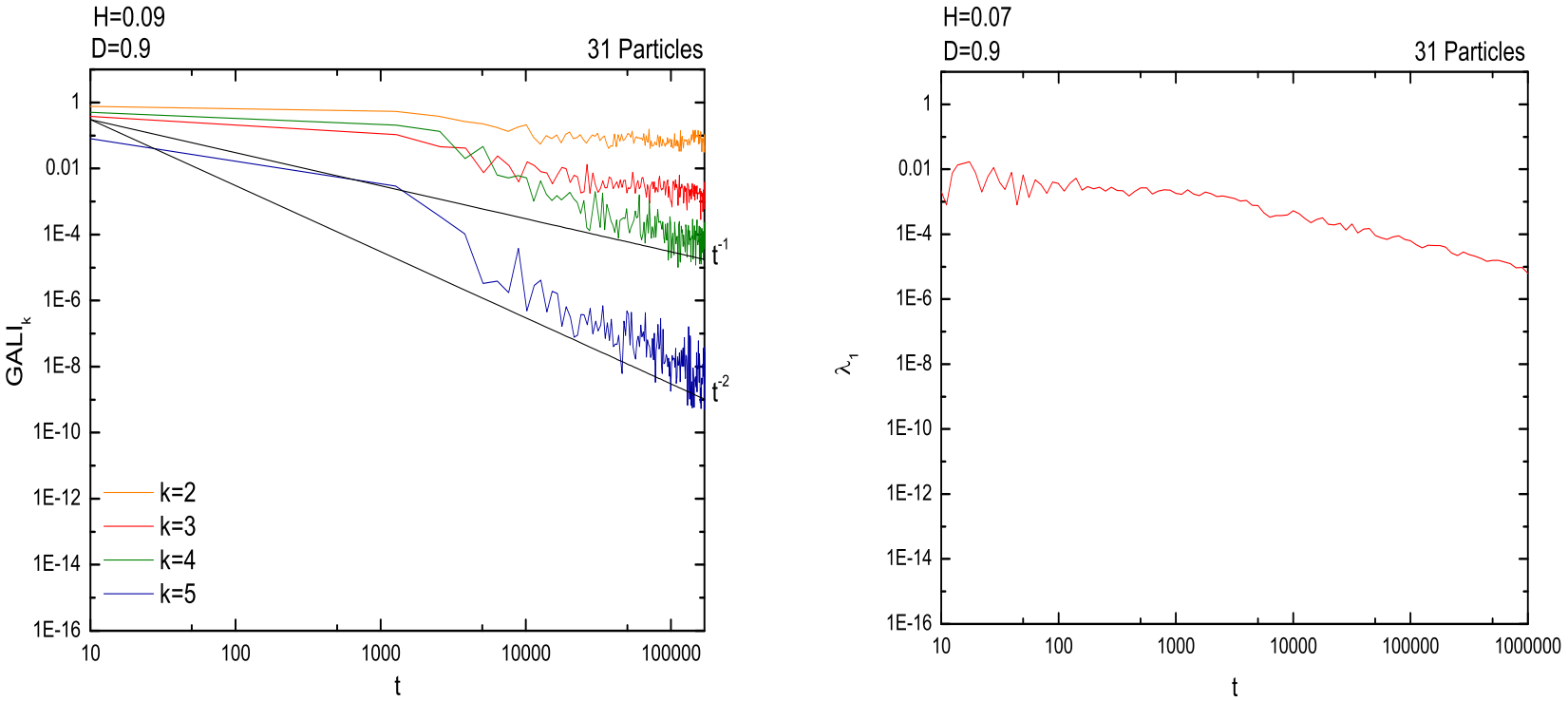

Figure 20: (a) One more experiment, with D=0.9 and N=31, in which the oscillations of the central particles of (41) exhibit **quasiperiodic** behavior on a 3-dimensional torus. (b) The maximal Lyapunov exponent decreases slowly and cannot be reliably used to show the character of the dynamics.

However, at initial conditions further away from the periodic breather, i.e. D=0.7, GALI_2 predicts slow diffusion by falling to zero exponentially:

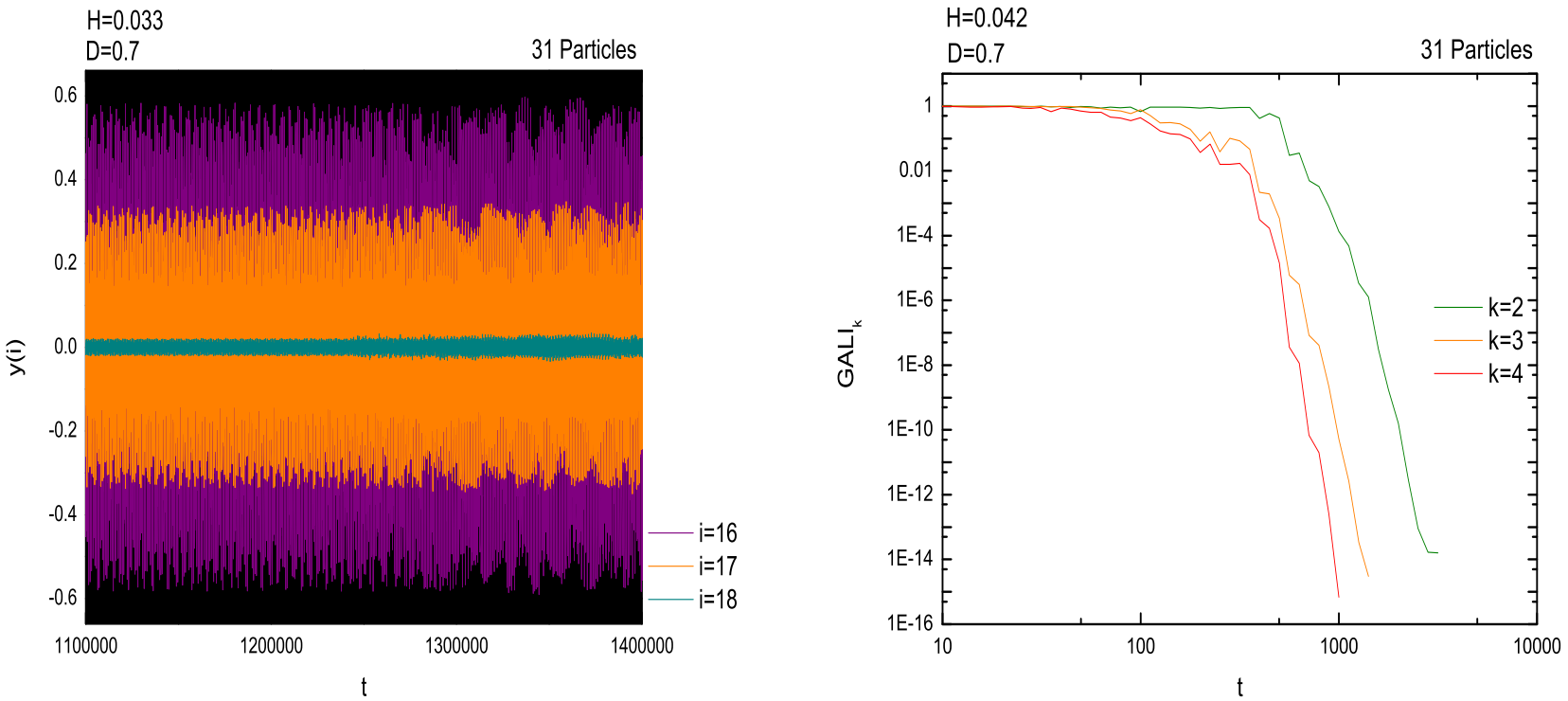

Figure 21:(a) The oscillations of the central particles of (41) with $N = 31$, **appear quasiperiodic** for very long times. (b) The solution, however, is **not on a torus** and diffuses slowly away, since even GALI_2 decays exponentially after about $t = 5000$.

On the Dynamics of N Weakly Coupled Standard Maps

The standard map, also referred to as the Chirikov–Taylor map, **but should also be called the Casati map**, is an area preserving map and appears in many physical problems. It is defined by the equations:

$$\begin{aligned} x_{n+1} &= x_n + y_{n+1}, \\ y_{n+1} &= y_n + K\sin(x_n), \end{aligned} \tag{42}$$

where both variables are taken modulo one on unit square. This map describes the motion of a simple mechanical system called a kicked pendulum. The variables x_n and y_n determine, respectively, the angular position of the pendulum and its angular momentum after the n^{th} kick. The constant K measures the intensity of the kicks.

Besides the kicked rotator, the standard map also describes other systems in the fields of mechanics of particles, accelerator physics, plasma physics, and solid state physics. However, this map is interesting from a fundamental point of view in physics and mathematics because it is a very simple model of a conservative system that displays hamiltonian chaos. It is therefore useful to study the development of chaos in this kind of systems.

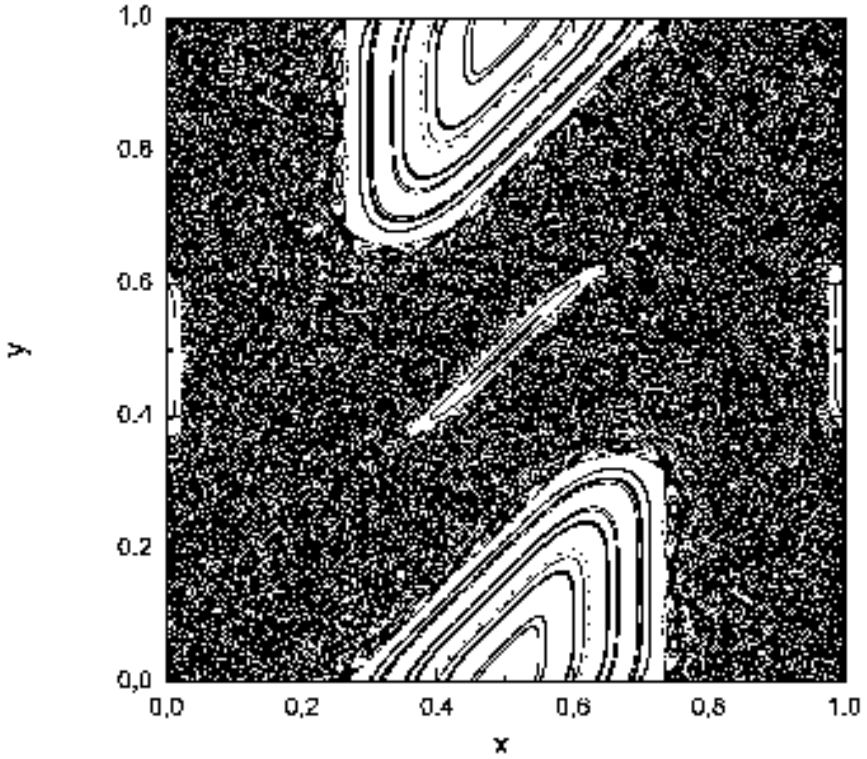

Figure 22: Poincaré surface of section of the standard map for $K = 2$. The stable point $(x, y) = (0.5, 0.0)$ is surrounded by a large regions of stability.

Let us now consider N coupled standard maps:

$$\begin{aligned} x^j_{n+1} &= x^j_n + y^j_{n+1}, \\ y^j_{n+1} &= y^j_n + \frac{K_j}{2\pi}\sin(2\pi x^j_n) - \frac{\beta}{2\pi}\{\sin[2\pi(x^{j+1}_n - x^j_n)] + \sin[2\pi(x^{j-1}_n - x^j_n)]\} \end{aligned} \tag{43}$$

with $j = 1, ..., N$ and $x_0 = x_{N+1} = y_0 = y_{N+1} = 0$.

I. In a series of FPU - like experiments, we changed to linear normal mode coordinates and placed initial conditions on some of these modes. As in the FPU case, for small coupling ($\beta = 0.0001$) there were recurrences between few modes. However, for larger value of the coupling ($\beta = 0.01$), recurrences break down and the orbits become chaotic.

II. In another experiment, with $K_j = 2$ and $\beta = 0.001$, we assumed that a stable periodic breather exists and chose initial conditions on a nearby localized solution, exciting only the 11th out of 20 coupled maps and found that the orbit lies on a 2D torus. Exciting the 11 and 12th particles, on the other hand, leads to motion that lies on a 3D torus.

I. The FPU Case: Keeping only the first (linear) term in the Taylor expansion of the $sine$–function in the equations of motion, we obtain the following linear system of equations:

$$x' = \mathcal{A} \cdot x, \tag{44}$$

where $x' = (x^1_{n+1}, y^1_{n+1}, ..., x^N_{n+1}, y^N_{n+1})^T$, $x = (x^1_n, y^1_n, ..., x^N_n, y^N_n)^T$.

Using well–known methods of linear algebra, we may diagonalize the matrix $\mathcal{A}$ if the eigenvalues λ_i are real and discrete.

In our case, however, we have oscillations about a stable equilibrium point, hence the above system has $2N$ discrete complex eigenvalues $\lambda_j = a_j + ib_j$, $\bar{\lambda}_j = a_j - ib_j$ and $w_j = u_j + iv_j$, $\bar{w}_j = u_j - iv_j$ are the corresponding eigenvectors with $j = 1, 2, ..., N$. Then $u_1, v_1, ..., u_N, v_N$ form a basis of the space $\mathcal{R}^{2N}$. The matrix $\mathcal{P} = [v_1, u_1, , ..., v_N, u_N]$ is invertible and leads to the Jacobi normal form:

$$\mathcal{B} = \mathcal{P}^{-1} \cdot \mathcal{A} \cdot \mathcal{P} = diag \begin{bmatrix} a_j & -b_j \\ b_j & a_j \end{bmatrix},$$

of a $2N \times 2N$ matric $\mathcal{B}$ with 2×2 blocks along its diagonal.

We thus reduce the initial problem to a system of uncoupled equations using the transformation $z = \mathcal{P}^{-1}x$ and its evolution is described by the following equations:

$$z' = \mathcal{P}^{-1} \cdot \mathcal{A} \cdot \mathcal{P} \cdot z, \tag{45}$$

where $z' = (l^1_{n+1}, k^1_{n+1}, ..., l^N_{n+1}, k^N_{n+1})^T$, $z = (l^1_n, k^1_n, ..., l^N_n, k^N_n)^T$. The z – coordinates describe the motion of the linear normal modes of the map. Thus, in order to excite a continuation of one or more of these modes, we extract the appropriate x – initial condition by the transformation $x = \mathcal{P} \cdot z$.

The evolution in the uncoupled coordinates is given by the transformation:

$$\begin{bmatrix} l^j_{n+1} \\ k^j_{n+1} \end{bmatrix} = \begin{bmatrix} a_j & -b_j \\ b_j & a_j \end{bmatrix} \cdot \begin{bmatrix} l^j_n \\ k^j_n \end{bmatrix}, \tag{46}$$

where each pair of (l_j, k_j) corresponds to a normal mode of the system. Since the map is area–preserving, $(a_j^2 + b_j^2) = 1$, where a quantity, we may define as the energy $E^j_n = (l^j_n)^2 + (k^j_n)^2$ is preserved under the evolution of the map, i.e. $E^j_{n+1} = E^j_n$.

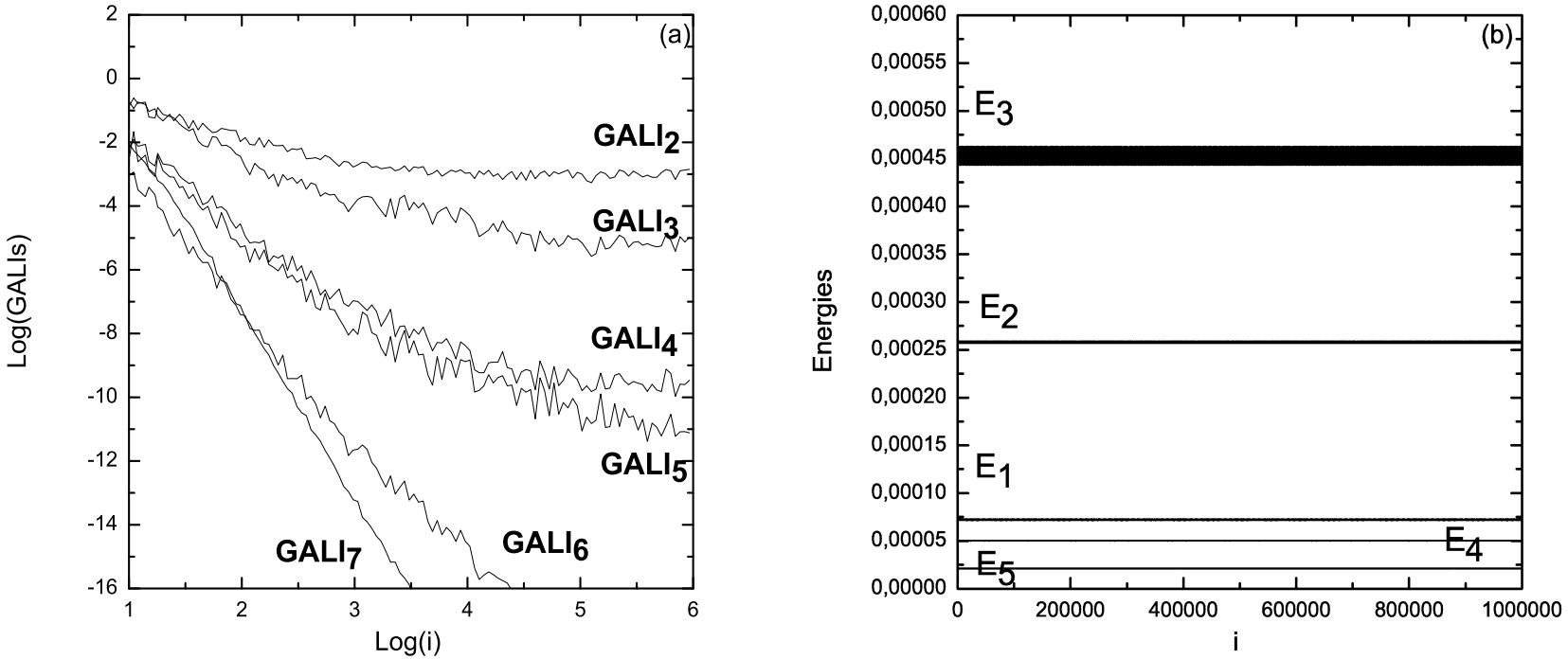

Figure 23: (a) GALIs for 5 coupled standard maps, with $K_1 = -2.30, K_2 = -2.35,$ $K_3 = -2.40, K_4 = -2.45, K_5 = -2.50$ and $\beta = 0.00001$ of an initial condition that excites all the 5 different normal modes. GALI$_{2,3,4,5}$ fluctuates around a non–zero value implying a regular motion that lies on a 5D torus. (b) The energies for the corresponding normal modes.

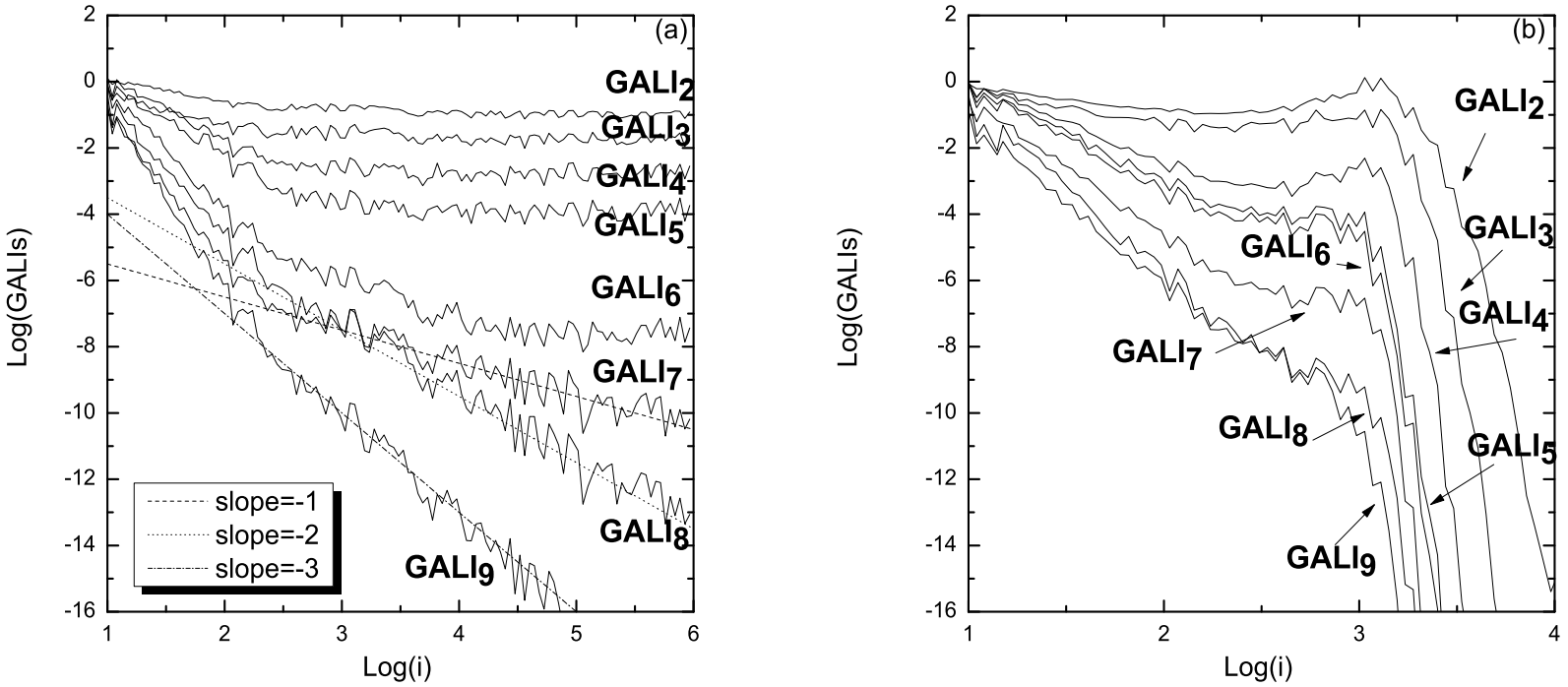

Figure 24:(a) GALIs for 20 coupled standard maps with $\beta = 0.00001$ and different K_i, where we have excited one normal mode. GALI$_{2,\ldots,6}$ asymptotically become constant implying a motion that lies on a 6D torus. (b) An orbit with the same initial condition and K_i as (a) but with larger value of the coupling ($\beta = 0.01$). The orbit has become now chaotic due to this increase and all the GALIs decay exponentially to zero.

II. The Breather Case:

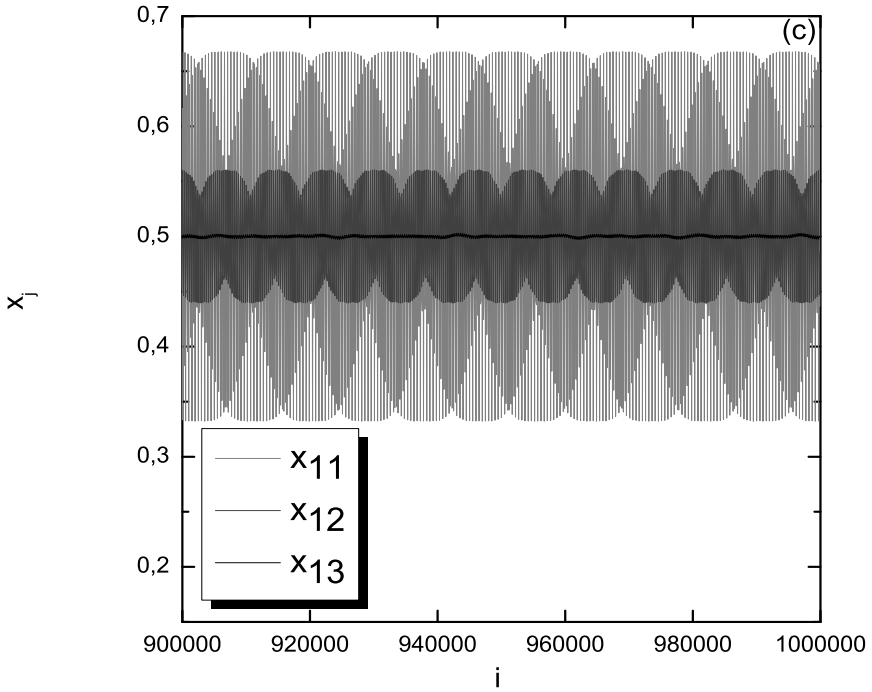

Figure 25: Amplitude oscillations Distance ranges of the 11^{th} (light gray color), 12^{th} (gray color)and 13^{th} (black color) of $N = 20$ – coupled standard maps with $K_j = 2$ and $\beta = 0.001$ for the initial conditions (R2): (x_j, y_j)=(0.5,0.0), $\forall\ j \neq 11, 12$ while $(x_{11}, y_{11}) = (0.65, 0.0)$, $(x_{12}, y_{12}) = (0.55, 0.0)$. We have plotted the last 10^5 iterations of the calculation.

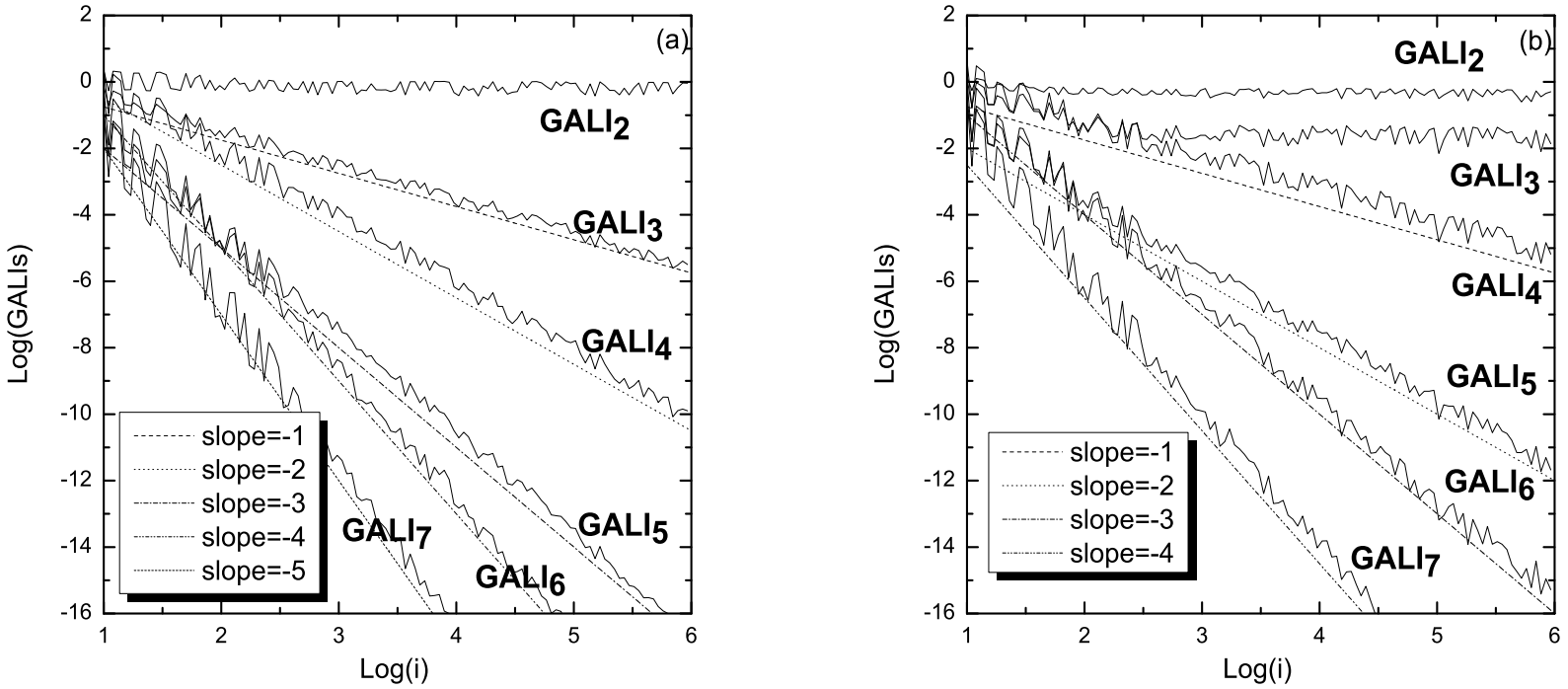

Figure 26:(a) The GALIs of the initial condition R1:(x_j, y_j)=(0.5,0.0), $\forall\ j \neq 11$ and $(x_{11}, y_{11}) = (0.65, 0.0)$, for $N = 20$ – coupled standard maps with $K_j = 2$ and $\beta = 0.001$, imply that the motion lies on a 2D torus, while (b) for the initial condition R2:(x_j, y_j)=(0.5,0.0), $\forall\ j \neq 11, 12$ while $(x_{11}, y_{11}) = (0.65, 0.0)$, $(x_{12}, y_{12}) = (0.55, 0.0)$, the motion lies on a 3D torus.

Conclusions

1) Generalizing the SALI method, we introduced the Generalized Alignment Indices, GALI$_k$. GALI$_k$ is the 'norm' of the 'exterior' or wedge product of k normalized deviation vectors and hence represents the 'volume' of a parallelepiped having as edges $k > 2$ initially independent deviation vectors.

We have shown that for chaotic orbits:

$$\text{GALI}_k(t) \propto e^{-[(\sigma_1-\sigma_2)+(\sigma_1-\sigma_3)+\cdots+(\sigma_1-\sigma_k)]t} . \quad (47)$$

while for ordered ones:

$$\text{GALI}_k(t) \sim \begin{cases} \text{constant} & \text{if } 2 \leq k \leq s \\ \frac{1}{t^{k-s}} & \text{if } s < k \leq 2N-s \\ \frac{1}{t^{2(k-N)}} & \text{if } 2N-s < k \leq 2N \end{cases} . \quad (48)$$

where s is the dimension of the torus and no deviation vectors are initially tangent to the torus.

2) The GALI$_k$s were successfully applied to:

a) Distinguish **chaotic orbits very rapidly**, for $2 \leq k \leq 2N$, **from ordered orbits** (GALI$_k$ decays exponentially or fluctuates around a constant)

b) Determine from the GALI$_k$ power law decays the **dimensionality** $s \leq N$ **of the subspace of ordered motion**, identifying **low - dimensional** tori

c) Predict **slow diffusion** of orbits toward a larger chaotic "sea", near **normal modes of the FPU lattice** as well as the breakdown of quasiperiodic motion near stable periodic breathers

d) Obtain analogous results for FPU - like recurrences and localized oscillations of **N coupled standard maps**, showing that GALI$_k$ are equally useful for analyzing the dynamics of $2N$–dimensional systems of **symplectic maps.**

References

1. T. Bountis, "Stability of Motion: From Lyapunov to N - Degree of Freedom Hamiltonian Systems", [2006], "Nonlinear Phenomena and Complex Systems", vol. **9**(3) ,209 -239.

2. Ch. Antonopoulos and T. Bountis [2006], ROMAI Journal **2**(2),1; E. Christodoulidi and T. Bountis [2006], ROMAI Journal **2**(2),37.

3. Skokos, Ch., Bountis, T. and Antonopoulos, Ch. [2007], “Geometrical properties of local dynamics in Hamiltonian systems: the Generalized Alignment Index (GALI) method”, Physica D **231**, 30.

4. Skokos, Ch., Bountis, T. and Antonopoulos, Ch. [2008], "Detecting Chaos, Determining the Dimensions of Tori and Predicting Slow Diffusion in FPU Lattices by the Generalized Alignment Index method", to appear in European Physics Journal - Special Edition dedicated to Celso Grebogi’s birthday.

5. Bountis T., Manos Th., Christodoulidi E., [2008] "Applications of the GALI Method to Localization in Nonlinear Systems", J. of Comput. and Appl. Math., to appear.